Optimization of the solid ISOL method for volatile reaction products of heavy ion beam reactions

International Remote Student Training at

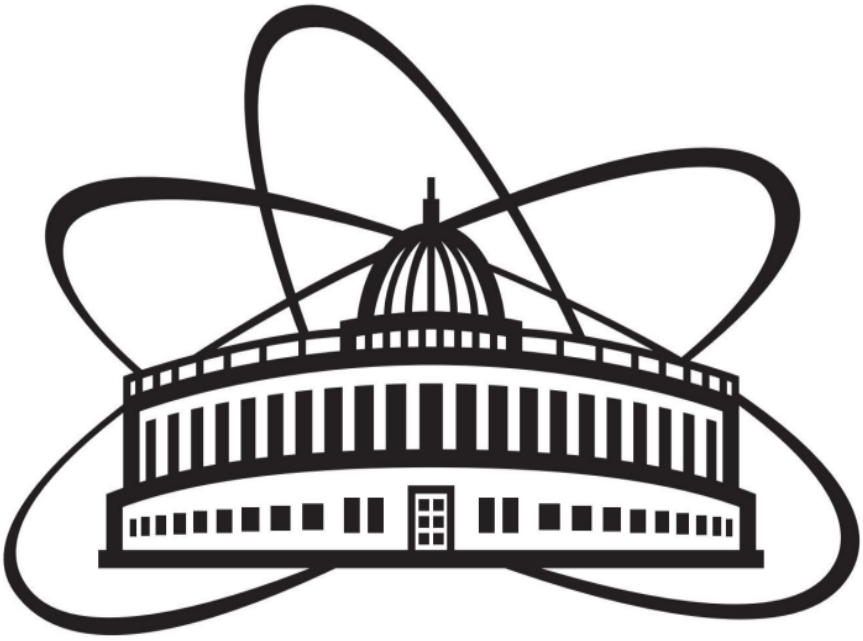

Joint Institute for Nuclear Research

Scientific Supervisor

Mr Viacheslav Vedeneev

Student

Remadhu Gowri S

1. ABSTRACT

This project is mainly aimed on the data analysis of the solid-state ISOL system employed at the MASHA mass separator for the optimal separation of volatile reaction products obtained in heavy ion beam reactions. Three reactions were studied: $^{40}Ar + ^{166}Er$, $^{40}Ar + ^{148}Sm$, and $^{48}Ca + ^{242}Pu$. These reactions give neutron-deficient isotopes of mercury and radon, the alpha-decay spectra of which were analyzed in detail. With stepwise plotting, peak fitting, and calibration procedures in OriginPro, decay chains were reconstructed, energy matrices were calibrated to produce insightful heat maps. Some of the important findings are the determination of peak locations, channel-to-energy calibration coefficients, and visualization of isotope distribution in detector strips. This study enhances understanding of the ISOL system's performance and assists future optimization activities in the detection of short-lived isotopes by utilizing solid-state catcher materials and high-temperature systems. All the analysis was carried out based on provided experimental data without undertaking experimental operations.

2. INTRODUCTION

The search for heavy and superheavy elements is still one of the most interesting and complicated fields in contemporary nuclear physics. The further extension of the periodic table makes advanced experimental methods and precise data analysis ever more important for recognition and description of these exotic and frequently short-lived nuclei. One of the techniques used in such research is the solid-state ISOL (Isotope Separation On-Line) method, which, when combined with sophisticated detection systems such as the MASHA (Mass Analyzer of Super Heavy Atoms) apparatus, enables scientists to effectively identify evaporation residues and their decay products from complete fusion reactions.

During this project, I concentrated only on the data analysis of experiments done through heavy ion beam reactions that involve the mentioned fusion systems of $^{40}Ar + ^{166}Er$, $^{40}Ar + ^{148}Sm$, and $^{48}Ca + ^{242}Pu$. These kinds of reactions have specific interest in the sense that they produce neutron-deficient isotopes like radon and mercury, which are well known because of their alpha decay characteristics as well as their volatility. The analyzed data were obtained from detectors mounted on the MASHA apparatus, which scans alpha spectra over several strips and offers raw matrix information for building energy-position distributions.

My top-level goal with analysis was the discovery and calibration of the isotopic alpha decay energies resulting from such reactions. It involved production and analysis of one-dimensional spectra of alpha distributions for isotopes ^{180}Hg to ^{185}Hg, ^{201}Rn to ^{205}Rn, and ^{212}Rn, ^{218}Rn, and ^{219}Rn as well as making two-dimensional heat maps from matrices and calibrating them. The calibration step implied finding the correspondence between the

actual alpha decay energy and the channel number, known from measured spectra reference peaks. By comparing the resultant decay energies with those of known nuclear decay schemes, I was able to label isotope identities and confirm the decay chains of reaction products.

The motivation for this analysis is the potential to optimize the solid ISOL technique by improved knowledge of the behavior and decay characteristics of volatile reaction products at high-beam intensities. The knowledge that can be extracted from such analyses is crucial in future target material developments, hot catcher geometry, and general separation efficiency within the MASHA experimental setup.

3. SETUP DESCRIPTION

The MASHA (Mass Analyzer of Super Heavy Atoms) setup plays a crucial role in the identification and analysis of heavy and superheavy nuclei. While I did not participate in the experimental setup, my analysis is based on data obtained using this system, which has undergone several upgrades in recent years. These upgrades include improvements to the target box, ion source, data acquisition system, beam diagnostics, and control mechanisms. These enhancements were made to improve thermal efficiency, ionization rates, and overall reliability under the high-radiation, high-temperature conditions typical of heavy ion experiments.

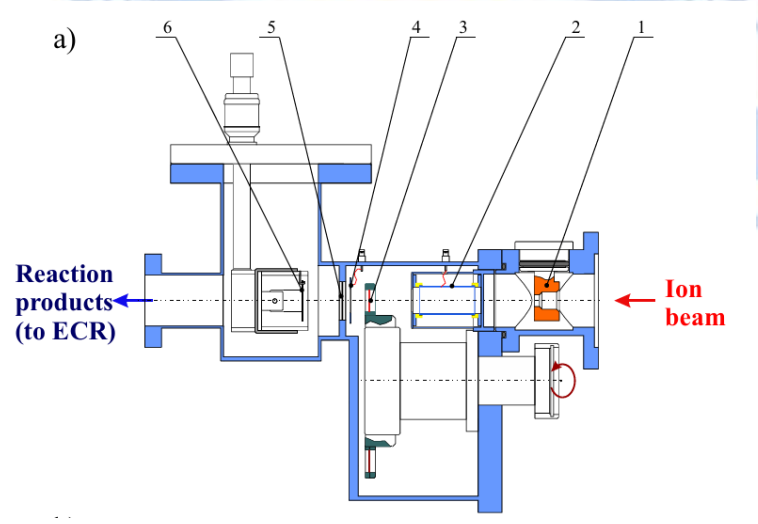

Fig. 1 Schematic overview of the target-hot catcher system. Here: 1– diaphragm; 2– pick-up sensor; 3 target on the wheel; 4– electron emission beam monitor; 5– separating foil; 6– hot catcher. b The photo of the rotating target cassette in assembly. 6 packs, 2 windows at 14 mm width each.

3.1 Target Box

The system uses a rotating target assembly enclosed within a block, offering advantages over a stationary design in terms of thermal distribution and irradiation efficiency. Targets are mounted on rotating discs operating at a frequency of 25 Hz, driven by a Siemens electric motor. This rotation allows for more uniform beam exposure and thermal management.

The heating system was also upgraded to utilize thermally expanded graphite, heated directly by electric current. This eliminated the need for indirect heating elements and improved uniformity. The separation foil was replaced with thin graphite due to its superior thermal tolerance compared to previously used titanium foils. These changes contribute to better thermal stability and resistance to radiation-induced degradation, ensuring more consistent separation performance.

3.2 Ion Source

The ion source operates using electron cyclotron resonance (ECR) principles under ultra-high frequency conditions, typically around 2.45 GHz. The reaction products enter the ion source as neutral atoms and are ionized to a +1 charge state. These ions are then accelerated to an energy of 38 keV using a three-electrode electrostatic lens system.

The ions are subsequently separated by a magnetic mass-to-charge (m/q) analyzer. Ionization efficiency for noble gases such as krypton and xenon reaches up to 90%, making these ideal candidates for system calibration and optimization. Mercury isotopes, which are chemically similar to the superheavy element Copernicium, are used in these experiments due to their volatile nature and behavior analogous to inert gases.

To minimize wall losses and enhance ionization efficiency, the inner surfaces of the ion source, catcher, and transport lines are coated with titanium nitride (TiN)**.** This chemically inert material has a low enthalpy of adhesion**,** meaning that volatile atoms like mercury have a reduced tendency to stick to it compared to bare stainless steel. As a result, atoms are less likely to be adsorbed on the walls, undergo fewer surface collisions**,** and have a higher probability of being transported and ionized efficiently.

Stable ion beam formation also depends on controlling several operational parameters. A helium buffer gas is introduced through a piezoelectric valve to maintain a chamber pressure of approximately $(1–2) \times 10^{-5}$ mbar. Under this condition, and with microwave power ranging from 20 to 60 W at 2.45 GHz, a stable plasma can be maintained. This setup yields beam currents of 600–700 μA when full wave absorption is achieved by the plasma chamber.

4. EXPERIMENTAL ANALYSIS AND DATA PROCESSING

4.1 Peak Analysis and Decay Interpretation

In the field of nuclear spectroscopy, the alpha decay spectra provide essential insight into the structure and stability of heavy nuclei. For this analysis, three complete fusion reactions were studied:

- **^{40}Ar + ^{148}Sm** producing isotopes ^{180}Hg to ^{185}Hg,
- **^{40}Ar + ^{166}Er** producing isotopes ^{201}Rn to ^{205}Rn,,
- **^{48}Ca + ^{242}Pu.** producing isotopes ^{212}Rn, ^{218}Rn, and ^{219}Rn.

In each case, the resulting nuclei undergo sequential alpha decay processes. The alpha particles emitted during these decays deposit specific energies in the detector medium, which manifest as distinct peaks in the resulting spectra. These peaks represent characteristic energies tied to specific isotopes and their decay transitions.

Understanding these spectra requires considering both the decay energy and the branching ratios, which describe the likelihood of a given decay path. Nuclides may exhibit multiple alpha decay paths with different energies and probabilities, leading to a spectrum with multiple peaks for a single isotope or its daughters. Furthermore, many heavy nuclei produce decay chains involving several subsequent alpha emissions, each of which appears in the spectral data.

For example, the reaction involving ^{40}Ar + ^{148}Sm produces neutron-deficient mercury isotopes. These nuclei lie near the proton drip line and often decay rapidly through alpha emission, contributing to a well-structured alpha energy spectrum. The presence of multiple isotopes, such as ^{180}Hg to ^{185}Hg, creates a complex profile of overlapping peaks that reflect the decay energies of both parents and their daughters.

In the reaction ^{40}Ar + ^{166}Er, radon isotopes ^{201}Rn to ^{205}Rn, are observed. These neutron-deficient radon nuclei provide a useful testing ground for alpha decay systematics in the heavy element region. The observed spectral features are shaped by their specific decay energies and the contributions from their daughter polonium and lead isotopes.

The third reaction, ^{48}Ca + ^{242}Pu., targets the synthesis of superheavy elements, with radon isotopes like ^{212}Rn, ^{218}Rn, and ^{219}Rn.

In each spectrum, the observed peaks were interpreted by comparison with established nuclear decay schemes. Known decay energies and branching ratios from nuclear databases were used to assign peak identities, confirming both the parent isotope and the decay mode. The presence of expected peaks corresponding to daughter products further supported the chain identification, allowing for confident isotope assignments.

The alpha energy spectra for all three reactions confirmed the presence of the expected isotopes, validated through energy correspondence with known decay chains. The analysis contributes to a broader understanding of the decay properties of neutron-deficient and superheavy nuclei and supports the identification of products in future heavy ion collision studies.

4.2 Heat Map Interpretation and Energy Calibration

Beyond the one-dimensional spectral lines, two-dimensional heat maps constructed from the matrix data of alpha events provide a spatially resolved view of nuclear activity. These visualizations reflect the intensity of decay events across a defined range of detection parameters, with the density and color variations correlating directly to the energy deposition profiles of decaying nuclei.

The heat maps offer an additional dimension to interpret the complexity of nuclear decay, particularly in heavy and superheavy element production, where overlapping alpha energies and high event rates can obscure interpretation in traditional spectra. They allow visual identification of high-density clusters associated with prominent alpha-emitting isotopes, while also revealing lower-intensity structures corresponding to rarer or shorter-lived decay events. This makes them exceptionally useful in distinguishing closely spaced alpha lines or verifying the presence of weakly populated decay channels.

Calibration of these maps is central to their interpretability. The raw detector response must be translated into physical alpha energies, a process achieved by anchoring known decay energies (from well-established reference isotopes) to their corresponding positions in the matrix. This linear correlation aligns the channel-based axis of the detector output with the true energy scale, effectively transforming the visual map into a calibrated tool for nuclear identification.

Each reaction system displayed its own distinct energy calibration. In the $^{40}Ar + ^{148}Sm$ system, the calibration allowed for precise mapping of alpha decay from ^{180}Hg to ^{185}Hg isotopes, whose energies span a tightly clustered range near 6.0–6.6 MeV. The calibration anchored these values, allowing for accurate placement of decay zones within the heat map.

For the $^{40}Ar + ^{166}Er$ system, covering the range of ^{201}Rn to ^{205}Rn,, the calibration extended slightly higher in energy, due to the increased mass and nuclear charge of the isotopes involved. This allowed for the resolution of a more dispersed set of decay events, including transitions with varying half-lives and branching ratios.

Finally, the $^{48}Ca + ^{242}Pu$. system required calibration over a broader and higher-energy range due to the production of isotopes such as ^{212}Rn, ^{218}Rn, and ^{219}Rn — products of a reaction pathway leading toward superheavy nuclei. These isotopes are key markers in identifying decay chains from elements near the predicted island of stability. The heat map for this system revealed well-defined clusters that traced known decay sequences, supporting the identification of multistep alpha-decay chains extending toward lighter daughter nuclei.

The properly calibrated and interpreted heat maps thus serve as both qualitative and quantitative indicators of nuclear behavior. They validate theoretical decay predictions and reinforce the structural interpretations derived from one-dimensional spectra — establishing a holistic view of the nuclear landscape produced in each heavy-ion reaction.

5. RESULTS AND DISCUSSION

The interpretation of alpha decay spectra plays a crucial role in understanding the structure of neutron-deficient and superheavy nuclei. The energy and intensity of alpha emissions are directly connected to nuclear shell effects, decay probabilities, and isotope formation paths in heavy-ion fusion reactions. Through analysis of alpha spectra, it is possible to identify isotopes by their decay signatures, deduce decay chains, and infer nuclear structure properties.

1. Reaction: $^{40}Ar + ^{148}Sm \rightarrow ^{180}\text{-}^{185}Hg$

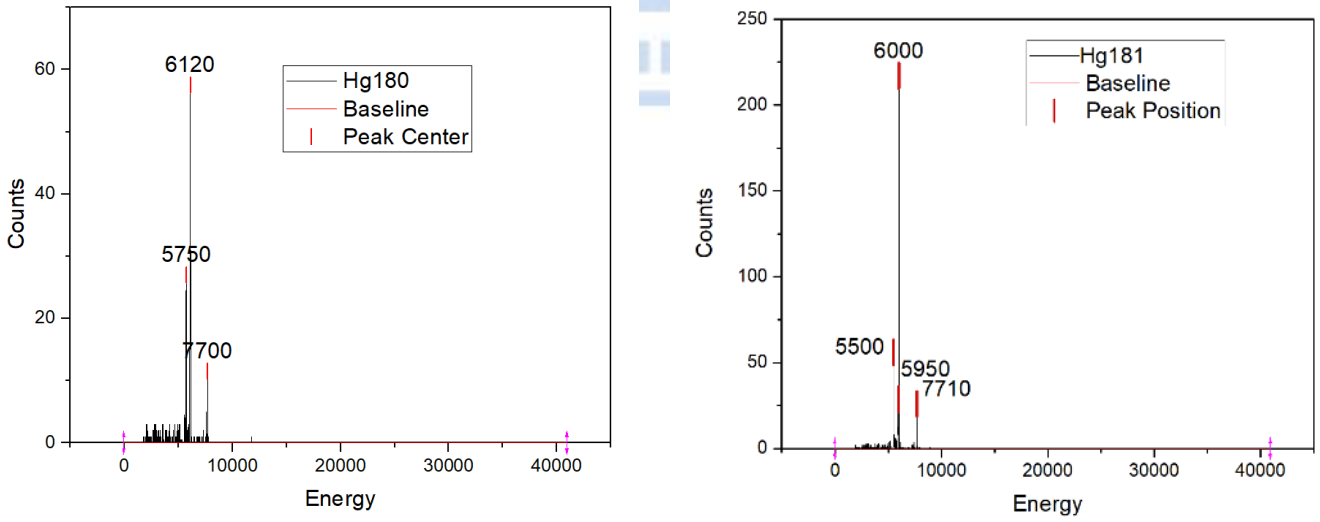

Figure 1&2: Alpha energy spectrum for reaction products of $^{40}Ar + ^{148}Sm$.

Hg180			
Detected Peak (keV)	**Isotope**	**Decay Energy (keV)**	**Branching Ratio (%)**
5750	Pt176	5753	99.74
6120	Hg180	6119	99.87

Hg181			
Detected Peak (keV)	**Isotope**	**Decay Energy (keV)**	**Branching Ratio (%)**
5500	Pt177	5517	88.5
5950	Hg181	5938	6.1
6000	Hg181	60006	87

Table 1&2: Summary of detected alpha peaks for $^{40}Ar + ^{148}Sm$, with corresponding isotope identification.

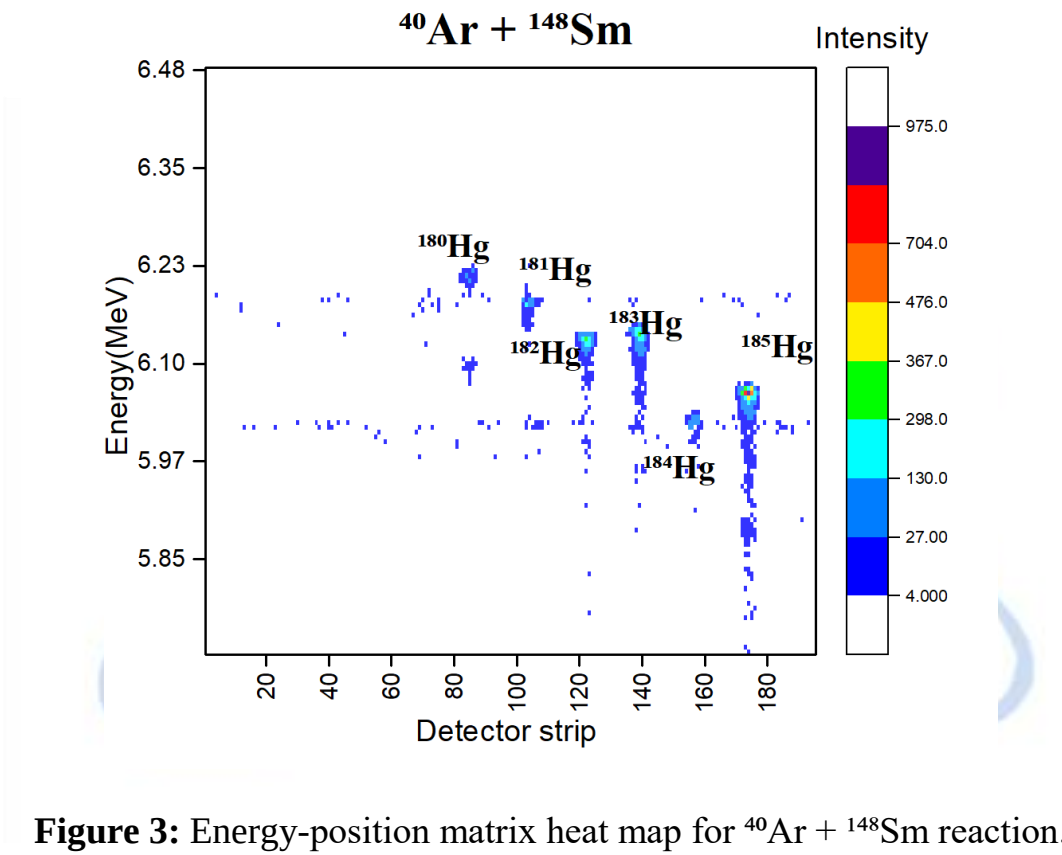

Figure 3: Energy-position matrix heat map for $^{40}Ar + ^{148}Sm$ reaction.

2. Reaction: $^{40}Ar + ^{166}Er \rightarrow ^{201-205}Rn$

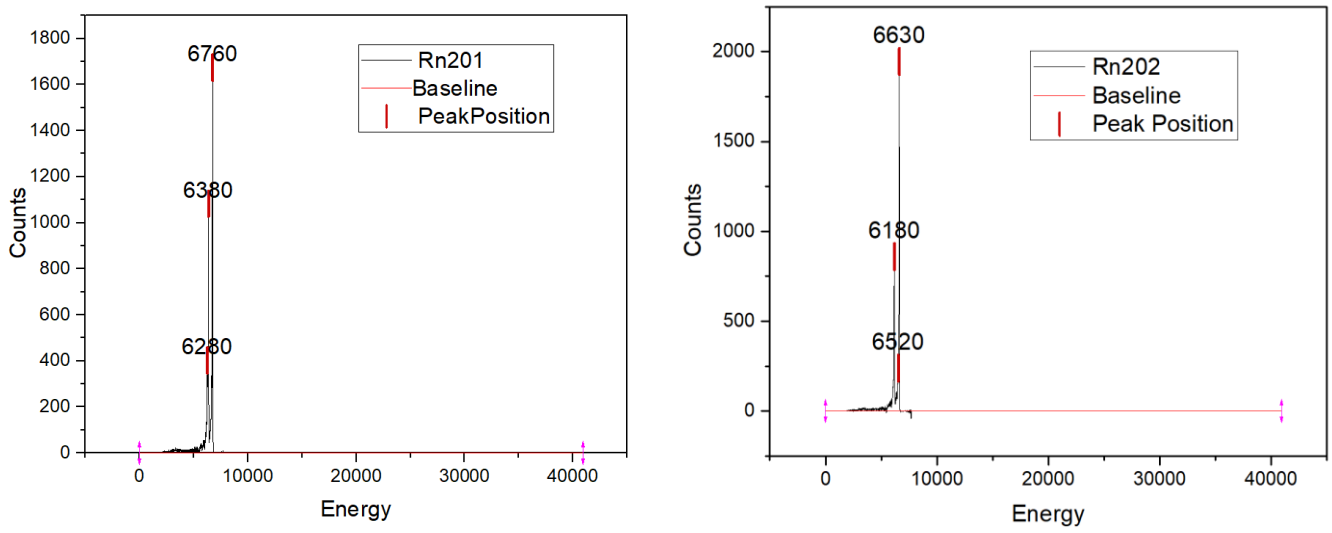

Figure 4&5: Alpha energy spectrum for reaction products of $^{40}Ar + ^{166}Er$.

Rn201			
Detected Peak (keV)	**Isotope**	**Decay Energy (keV)**	**Branching Ratio (%)**
6280	Po197	6281	100
6380	Po197	6383.4	99.3
6760	Rn201	6773	100

Rn202			
Detected Peak (keV)	**Isotope**	**Decay Energy (keV)**	**Branching Ratio (%)**
6180	Po198	6182	99.9987
6630	Rn202	6639.5	99.9982

Table 3&4: Summary of detected alpha peaks for $^{40}Ar + ^{166}Er$, with corresponding isotope identification.

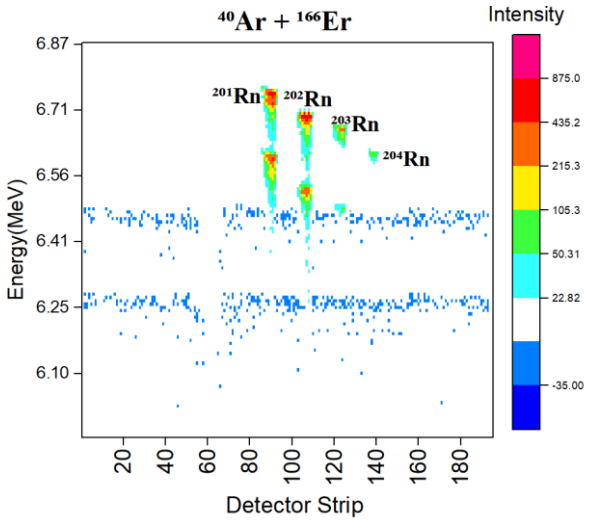

Figure 6: 2D heat map showing decay distribution for $^{40}Ar + ^{166}Er$.

3. Reaction: $^{48}Ca + ^{242}Pu \rightarrow ^{212}Rn, ^{218}Rn, ^{219}Rn$

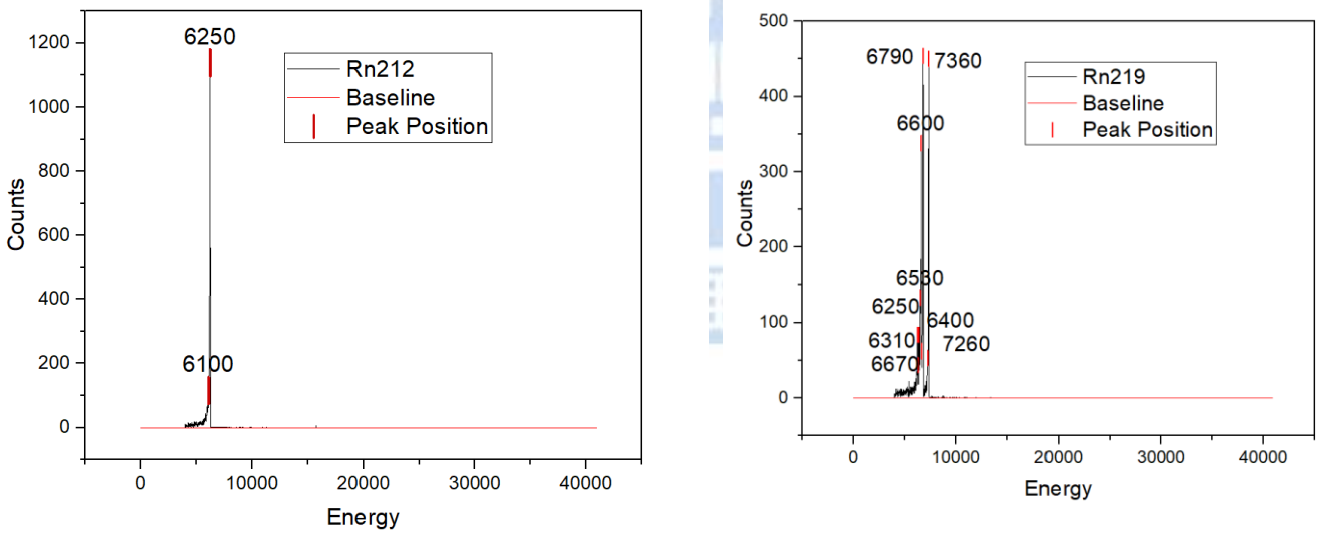

Figure 7&8: Alpha spectrum of reaction products from $^{48}Ca + ^{242}Pu$.

Rn212			
Detected Peak (keV)	**Isotope**	**Decay Energy (keV)**	**Branching Ratio (%)**
6100	Fr212	6127	1.14
6250	Rn212	6264	99.95

Rn219			
Detected Peak (keV)	**Isotope**	**Decay Energy (keV)**	**Branching Ratio (%)**
6250	Rn219	6223	0.004
6310	Rn219	6211	0.054
6400	Pa227	6401.7	9.4
6499	Rn219	6502	0.12

Table 5&6: List of identified peaks in the $^{48}Ca + ^{242}Pu$ reaction, showing decay energies and isotope assignments.

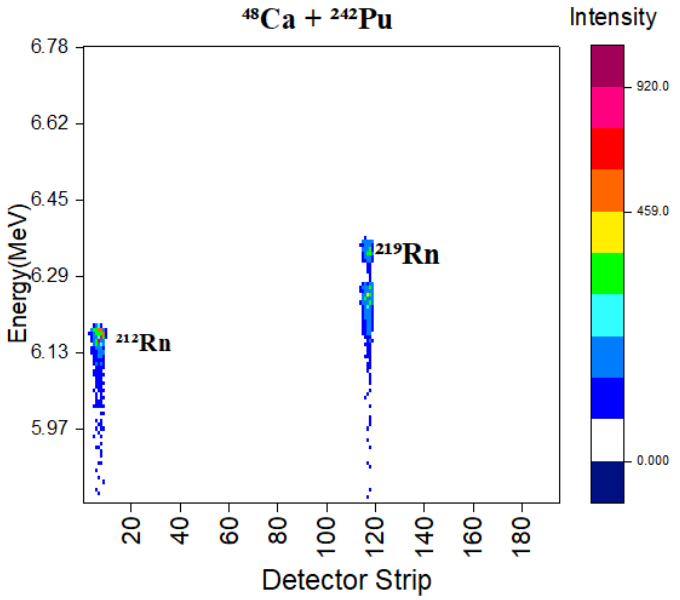

Figure 9: Energy-position matrix heat map for $^{48}Ca + ^{242}Pu$.

6. CONCLUSION

This analysis provided a detailed study of alpha decay signatures resulting from three heavy-ion fusion reactions: $^{40}Ar + ^{148}Sm$, $^{40}Ar + ^{166}Er$, and $^{48}Ca + ^{242}Pu$. By examining one-dimensional alpha energy spectra and calibrated heat maps, isotopic identifications were made for nuclei in the mercury and radon regions, ranging from ^{180}Hg to ^{185}Hg, ^{201}Rn to ^{205}Rn, and ^{212}Rn, ^{218}Rn, and ^{219}Rn. Each alpha peak was carefully matched to known decay energies, allowing confident assignment of isotopes and their respective decay chains.

The calibration of alpha spectra through known reference energies enabled precise determination of energy-channel relationships, making it possible to trace and confirm the nuclear processes involved in the reactions. The results contribute to ongoing efforts in mapping nuclear properties near the proton drip line and in the transuranium region. The analysis confirms that alpha spectroscopy remains a powerful tool for identifying short-lived nuclei and validating the formation of isotopes produced via complete fusion reactions. These findings form a reliable basis for future studies on the synthesis and detection of superheavy elements.

7. REFERENCES

1. Dmitriev, S. N., Oganessyan, Yu. Ts., Utyonkov, V. K., Shishkin, S. V., Eremin, A. V., Lobanov, Yu. V., Tsyganov, Yu. S., Chepygin, V. I., Sokol, E. A., Vostokin, G. K., Aksenov, N. V., Hussonnois, M., Itkis, M. G., Gäggeler, H. W., Schumann, D., Bruchertseifer, H., Eichler, R., Shaughnessy, D. A., Wilk, P. A., Kenneally, J. M., Stoyer, M. A., & Wild, J. F. (Chemical Identification of Dubnium as a Decay Product of Element 115 Produced in the Reaction $^{48}Ca + {}^{243}Am$).

2. Chernysheva, E. V., Rodin, A. M., Dmitriev, S. N., Gulyaev, A. V., Komarov, A. B., Novoselov, A. S., Oganessian, Yu. Ts., Podshibyakin, A. V., Salamatin, V. S., Stepantsov, S. V., Vedeneev, V. Yu., & Yukhimchuk, S. A. (Determination of separation efficiency of the mass-spectrometer MASHA by means of measurement of absolute cross-sections of evaporation residues).

3. Rodin, A. M., Chernysheva, E. V., Dmitriev, S. N., Gulyaev, A. V., Kamas, D., Kliman, J., Krupa, L., Novoselov, A. S., Oganessian, Yu. Ts., Opíchal, A., Podshibyakin, A. V., Salamatin, V. S., Stepantsov, S. V., Vedeneev, V. Yu., & Yukhimchuk, S. A. (Features of the solid-state ISOL method for fusion evaporation reactions induced by heavy ions).

4. Gäggeler, H. W. (Mendeleev's Principle Against Einstein's Relativity: News from the Chemistry of Superheavy Elements).

5. Eichler, R., Aksenov, N. V., Belozerov, A. V., Bozhikov, G. A., Chepigin, V. I., Dmitriev, S. N., Dressler, R., Gäggeler, H. W., Gorshkov, V. A., Haenssler, F., Itkis, M. G., Laube, A., Lebedev, V. Ya., Malyshev, O. N., Oganessian, Yu. Ts., Petrushkin, O. V., Piguet, D., Rasmussen, P., Shishkin, S. V., Shutov, A. V., Svirikhin, A. I., Tereshatov, E. E., Vostokin, G. K., Wegrzecki, M., & Yeremin, A. V. (Chemical Characterization of Element 112).

6. Vedeneev, V. Yu., Rodin, A. M., Krupa, L., Belozerov, A. V., Chernysheva, E. V., Dmitriev, S. N., Gulyaev, A. V., Gulyaeva, A. V., Kamas, D., Kliman, J., Komarov, A. B., Motycak, S., Novoselov, A. S., Salamatin, V. S., Stepantsov, S. V., Podshibyakin, A. V., Yukhimchuk, S. A., Granja, C., & Pospisil, S. (The Current Status of the MASHA Setup).

7. Веденеев, В. Ю., Родин, А. М., Крупа, Л., Камас, Д., Чернышева, Е. В., Гуляев, А. В., Голик, М., Климан, Я., Комаров, А. Б., Новоселов, А. С., Опихал, А., Пехоушек, Й., Подшибякин, А. В., Саламатин, В. С., Степанцов, С. В., Юхимчук, С. А. (2020). *Сечения образования испарительных остатков реакций полного слияния 144Sm(40Ar, xn)184–xHg, 148Sm(36Ar, xn)184–xHg, 144Nd(40Ca, xn)184–xHg*.